

# A Multiomics Study of Circulating Proteins and Kidney Stone Risk

Le-Ting Zhou<sup>1,2</sup>, Isaac W. Stark<sup>1,2,3</sup>, Muthuvel Jayachandran<sup>1,2</sup>, Peter C. Harris<sup>1,2</sup>, Andrew D. Rule<sup>1,2</sup>, Kevin Koo<sup>1,4</sup>, Shannon K. McDonnell<sup>1,5</sup>, Nicholas B. Larson<sup>1,5</sup>, and John C. Lieske<sup>1,2,6</sup>

## Key Points

- Circulating proteins independently associated with kidney stone diagnosis are related to kidney stone matrix.
- Lower circulating uromodulin and higher scavenger receptor cysteine-rich domain-containing group B protein levels were associated with higher kidney stone risk, whereas kidney stone presence elevates plasma matrix metalloproteinase 7 level.
- The protective effect of uromodulin against kidney stones was independent of kidney function.

## Abstract

**Background** Kidney stones are increasingly recognized as a systemic disorder with a high global prevalence. However, large proteomics studies are lacking.

**Methods** An individual-level proteomics study with rigorous adjustments was performed on 35,331 UK Biobank participants to uncover the independent associations between 2922 circulating proteins and prevalent kidney stone disease. Mendelian randomization analysis was used to assess causal relationships. Findings were validated using genomic data from the Mayo Clinic Biobank ( $N=43,744$ ), concentration-response analysis, transcriptomics analyses, and additional genome-wide association studies.

**Results** Nine plasma proteins were independently associated with a kidney stone diagnosis, including reduced uromodulin (UMOD;  $\beta$ ,  $-0.10$ ; 95% confidence interval [CI],  $-0.15$  to  $-0.05$ ) and elevated scavenger receptor cysteine-rich domain-containing group B protein (SSC4D;  $\beta$ ,  $0.28$ ; 95% CI,  $0.17$  to  $0.38$ ) and were enriched in extracellular matrix pathways. Mendelian randomization analysis revealed that the presence of kidney stone contributed to elevated levels of matrix metalloproteinase 7. Conversely, lower plasma UMOD (odds ratio [OR],  $0.93$ ; 95% CI,  $0.90$  to  $0.97$ ) and higher plasma SSC4D (OR,  $1.10$ ; 95% CI,  $1.02$  to  $1.18$ ) were associated with kidney stone risk. These associations were consistently replicated in the Mayo Clinic Biobank dataset (UMOD; OR,  $0.92$ ; 95% CI,  $0.86$  to  $0.98$ ; SSC4D; OR,  $1.13$ ; 95% CI,  $1.01$  to  $1.27$ ) and further validated by a concentration-response analysis. Single-nucleus RNA sequencing and quantitative trait loci analyses confirmed consistent associations between thick ascending limb UMOD expression and stone former status and with blood and urine UMOD concentrations. Genome-wide association study analysis, adjusted for eGFR, suggested that the protective role of UMOD against kidney stones was independent of kidney function.

**Conclusions** This study highlights significant associations between concentrations of specific blood proteins and a history of kidney stones. Several implicated proteins are related to kidney stone matrix, with UMOD independently associated with lower risk and SSC4D with higher risk of kidney stones.

JASN 00: 1–13, 2025. doi: <https://doi.org/10.1681/ASN.0000000768>

<sup>1</sup>Department of Nephrology, The Affiliated Wuxi People's Hospital of Nanjing Medical University, Wuxi, China and Wuxi Medical Center, Nanjing Medical University, Wuxi People's Hospital, Wuxi, China

<sup>2</sup>Division of Nephrology and Hypertension, Department of Medicine, Mayo Clinic, Rochester, Minnesota

<sup>3</sup>Department of Biological Sciences, Bethel University, Saint Paul, Minnesota

<sup>4</sup>Department of Urology, Mayo Clinic, Rochester, Minnesota

<sup>5</sup>Division of Biomedical Statistics and Informatics, Department of Health Sciences Research, Mayo Clinic, Rochester, Minnesota

<sup>6</sup>Department of Laboratory Medicine and Pathology, Mayo Clinic, Rochester, Minnesota

**Correspondence:** Dr. John C. Lieske, email: [Lieske.John@mayo.edu](mailto:Lieske.John@mayo.edu)

**Received:** January 3, 2025 **Accepted:** June 24, 2025

**Published Online Ahead of Print:** June 27, 2025

L-T.Z. and I.W.S. contributed equally to this work.

## Introduction

Kidney stone disease is a major health problem in both developed and underdeveloped countries worldwide that is increasing in prevalence, currently ranging between 1% and 13%.<sup>1</sup> Approximately 80%–90% of prevalent kidney stones are composed of calcium oxalate.<sup>2,3</sup> Kidney stone risk has been associated with several major medical conditions including hypertension, type 2 diabetes, CKD, and cardiovascular diseases,<sup>4–7</sup> with recent annual health care expenditures exceeding \$10 billion in the United States alone.<sup>1,8</sup>

Proteomic analyses of urine, blood, and kidney stone matrix have been used in prior small-scale observational studies to explore the mechanisms underlying stone pathogenesis. Pan *et al.* reported that more than 160 plasma proteins were dysregulated in patients with kidney stone compared with controls, with the majority involved in immune responses.<sup>9</sup> Similarly, Kovacevic *et al.* identified 17 urinary proteins, including osteopontin/secreted phosphoprotein 1 (SPP1) and syndecan-1, that were significantly downregulated in children with kidney stones compared with controls.<sup>10</sup> Proteomics analysis of 17 kidney stones identified uromodulin (UMOD) and albumin as the most prevalent proteins, irrespective of crystal composition.<sup>11</sup> To overcome the limitations of current cross-sectional studies, such as small sample sizes and the inability to establish causation, several proteome-wide Mendelian randomization (MR) studies using summary statistics have also been conducted recently.<sup>12,13</sup> However, the absence of individual-level data, lack of validation, and insufficient adjustment for comorbidities increase the risk of false associations, making these studies less rigorous than those using individual-level data for robust multivariable analyses.

To address these concerns, this study used a comprehensive multiomics approach, integrating individual-level proteomic data from the UK Biobank (UKBB) and genomic data from the Mayo Clinic Biobank (MCBB), to evaluate independent associations between plasma proteins and kidney stone formation. Our study aims to enhance understanding regarding the role of plasma proteins in kidney stone pathogenesis and provide a stronger foundation for future research into molecular mechanisms, prognosis, and treatment strategies.

## Methods

### Proteomics Study in the UKBB

The participants and study workflow are detailed in [Figure 1](#). Individual-level health and genetic data were obtained from more than 500,000 UKBB participants age 40–69 years at the time of recruitment after obtaining the necessary UKBB approvals (project ID 130923). Diagnoses were identified using the International Classification of Diseases, 10th Revision (ICD-10). Informed consent was obtained from all UKBB participants before data collection, and this study received Mayo Clinic institutional review board approval. More detailed information about the UKBB can be found at <https://www.ukbiobank.ac.uk/>.

The current proteomics study analyzed data for 2922 blood proteins measured using the Olink Proximity Extension

Assay in 35,331 UKBB participants. Plasma samples were collected both before and after kidney stone diagnosis, and the full list of proteins is available at <https://www.synapse.org/Synapse:syn52364558>. Individuals with possible active infection were excluded to minimize potential confounding using International Classification of Diseases codes as listed in the [Supplemental Methods](#). Proteins were quantified using the Normalized Protein eXpression method, a relative quantification technique that normalizes concentrations against a predefined calibration curve on a log<sub>2</sub> scale to ensure consistency and reliability across different samples. As reported by the UKBB Pharma Proteomics Project, the median interassay coefficient of variation for Olink control samples was <11%.<sup>14</sup>

A systematic approach was used to identify common comorbidities (present in >500 participants) that were associated with a kidney stone diagnosis (ICD-10 code: N20). Associations between the traits of interest and medical conditions were investigated *via* logistic regression models adjusted for age and sex, with significant associations defined by an odds ratio (OR) >1 and a Bonferroni-adjusted  $P < 0.05$ .

A stepwise approach was used, with unadjusted analysis for initial screening followed by multivariable analysis to identify proteins independently associated with kidney stones. The multivariable linear models were adjusted for age, sex, total cholesterol, HDL, uric acid, eGFR, body mass index (BMI), smoking, and 14 nonurinary system comorbidities ([Supplemental Table 1](#)). Proteins were considered significantly dysregulated in the context of kidney stones if they met the criteria of a Bonferroni-adjusted  $P < 0.05$  and an absolute log<sub>2</sub>-fold change (FC) >0.07, which corresponds to an absolute concentration difference of >5% compared with non-stone-forming controls, in both unadjusted and multivariable analyses.

### Genome-Wide Association Study

The basic characteristics of the genome-wide association study (GWAS) are presented in [Table 1](#). Informed consent and institutional review board/medical ethics approval were previously obtained by the individual cohort investigators. A genome-wide significance threshold of  $P < 5 \times 10^{-8}$  was applied to all GWAS analysis.

### UKBB

The standard blood protein GWAS data were sourced from the UKBB Pharma Proteomics Project.<sup>14</sup> Other GWAS analyses, including the standard kidney stone GWAS and additional eGFR-adjusted analyses, were performed using UKBB array data as part of project ID 130923. The array data were converted from GRCh37 to GRCh38 using Picard LiftOverVcf (<https://broadinstitute.github.io/picard/>). The following criteria were applied to ensure sample quality control and robustness of the data: (1) concordance between reported sex and genetic sex; (2) participants of White British ancestry; (3) exclusion of individuals with sex chromosome aneuploidy; and (4) inclusion of only nonrelated individuals. Quality control of variants and imputed data was conducted using PLINK2, with the parameters set to (`--mac 10 --maf 0.0001 --hwe 1e-15`

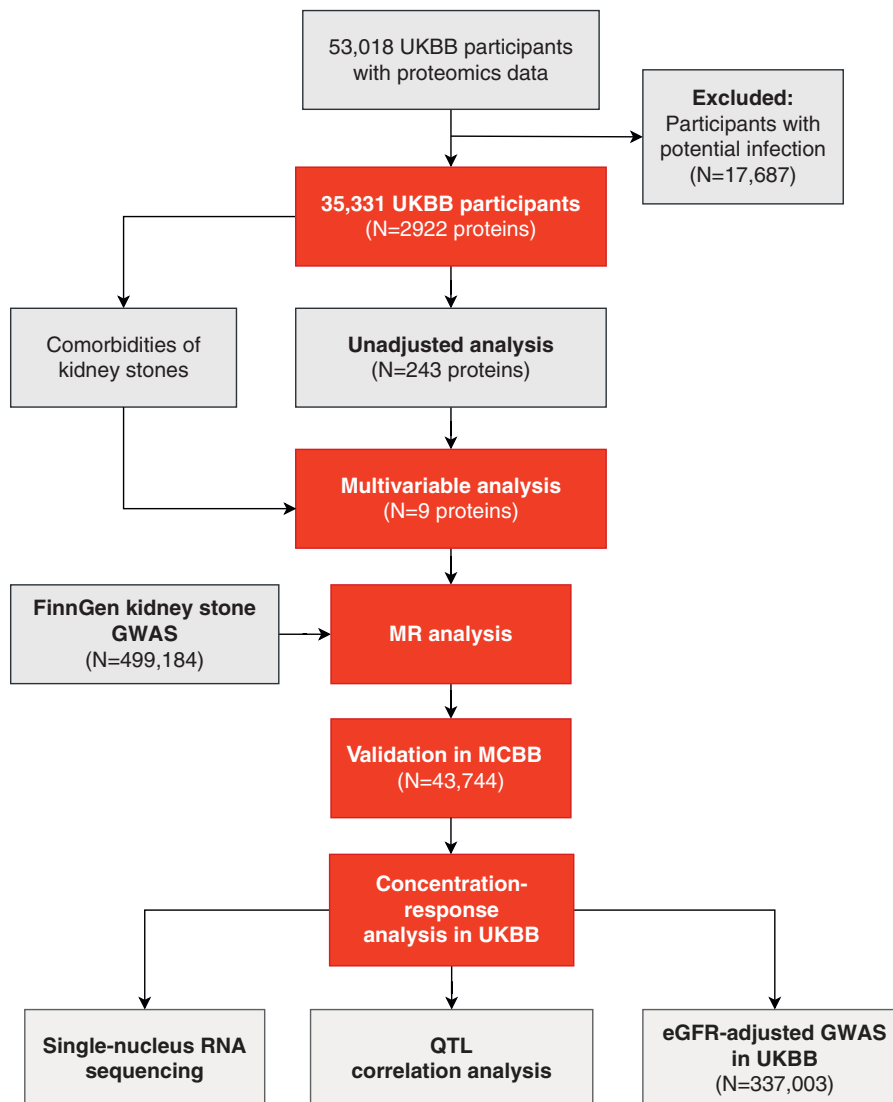


**Figure 1. Overall workflow of the study.** GWAS, genome-wide association study; MCBB, Mayo Clinic Biobank; MR, Mendelian randomization; QTL, quantitative trait locus; UKBB, UK Biobank.

--mind 0.1 --geno 0.1).<sup>15</sup> GWAS was executed with regenie, which employed a two-step process of whole-genome modeling followed by single-variant association testing.<sup>16</sup> The second step included the Firth approximation and an additive test, adjusting for sex, age, the top ten principal components of ancestry (as recommended by the UKBB Research Analysis Platform [<https://dnanexus.gitbook.io/uk-biobank-rap>]), and eGFR calculated according to the 2021 CKD Epidemiology Collaboration creatinine equation when appropriate.<sup>17</sup>

#### MCBB

Diagnostic and procedure codes for the MCBB participants were obtained from all Rochester Epidemiology Project sources, including the Mayo Clinic electronic health record. Both the kidney stone phenotype and controls were identified using electronic and surgical codes. The final MCBB cohort comprised 5998 kidney stone cases and 37,745 controls, all of European ancestry. GWAS was also executed

with regenie, using the Firth approximation and an additive test, adjusting for sex, age, and the top 13 principal components of ancestry, which together explained over 80% of cumulative genetic variance.<sup>16</sup> Comprehensive details regarding the genotyping method and the electronic definition of cases and controls are provided in the [Supplemental Methods](#).

#### Other GWAS Summary Statistics

The standard kidney stone GWAS summary statistics used in the MR analysis was sourced from FinnGen (DF12, released on November 4, 2024),<sup>18</sup> and the urinary UMOD GWAS from a meta-GWAS of 29,315 individuals from 13 cohorts.<sup>19</sup>

#### Linkage Disequilibrium Clumping, Protein Quantitative Trait Locus Identification, and Colocalization Analysis

The PLINK2 software was used to perform linkage disequilibrium clumping on the GWAS results as indicated.<sup>15</sup>

**Table 1. Characteristics of the genome-wide association study**

Traits	Resources	No. of Cases	No. of Controls	Total Sample Size	Ancestry
<b>Kidney stones<sup>a</sup></b>					
Kidney stones	UKBB	6368	330,635	337,003	European
Kidney stones (eGFR-adjusted)	UKBB	6071	315,059	321,130	European
Kidney stones	MCBB	5998	37,746	43,744	European
Kidney stones	FinnGen	12,999	486,185	499,184	European
<b>Blood protein levels</b>					
DDC	UKBB	—	—	33,628	European
GAL	UKBB	—	—	33,848	European
MMP7	UKBB	—	—	32,981	European
NPPC	UKBB	—	—	33,657	European
S100G	UKBB	—	—	33,874	European
SPP1	UKBB	—	—	34,028	European
SSC4D	UKBB	—	—	33,628	European
STC1	UKBB	—	—	33,962	European
UMOD	UKBB	—	—	34,030	European
UMOD (eGFR-adjusted)	UKBB	—	—	33,833	European
<b>Urinary protein levels</b>					
UMOD	Meta-analysis of 13 cohorts	—	—	29,315	European
UMOD/creatinine ratio	Meta-analysis of 13 cohorts	—	—	29,315	European

DDC, dopa decarboxylase; GAL, galanin; MCBB, Mayo Clinic Biobank; MMP7, matrix metalloproteinase 7; NPPC, natriuretic peptide C; S100G, S100 calcium-binding protein G; SPP1, secreted phosphoprotein 1 (also known as osteopontin); SSC4D, scavenger receptor cysteine-rich domain-containing group B protein; STC1, stannocalcin 1; UKBB, UK Biobank; UMOD, uromodulin.

<sup>a</sup>Kidney stone diagnoses were identified by International Classification of Diseases, 10th Revision code N20 in UK Biobank and FinnGen, whereas Mayo Clinic Biobank used combined diagnostic and procedure codes from the Rochester Epidemiology Project.

The reference panel for this analysis was composed of European patients from the 1000 Genomes Project. Cis-protein quantitative trait locus (pQTLs) were defined as loci with a significant effect on blood protein levels ( $P < 5 \times 10^{-8}$ ) and located within  $\pm 500$  kb of the encoding gene. Colocalization analysis was conducted using the coloc R package.<sup>20</sup> Posterior alignment probabilities (PPH4) were examined, with a threshold of  $\geq 0.7$  indicating significant colocalization.

### Enrichment Analysis

The enrichment analysis was conducted in R using clusterProfiler (v3.12.0).<sup>21</sup> Specifically, Kyoto Encyclopedia of Genes and Genomes and Reactome pathway queries were performed using the Kyoto Encyclopedia of Genes and Genomes pathway module and ReactomePA, respectively. A hypergeometric test was used for the enrichment analysis. A Benjamini–Hochberg adjusted  $P < 0.05$  was considered statistically significant.

### Two-Sample Bidirectional MR

This two-sample MR study was reported according to the Strengthening the Reporting of Observational Studies in Epidemiology Using MR statement.<sup>22</sup> All MR analyses were performed using the TwoSampleMR package in R.<sup>23</sup> Ideal instrumental variables satisfied the three core assumptions (relevance, independence, and exclusion restriction). In this study, single-nucleotide polymorphisms (SNPs) independently exhibiting strong associations with the traits of interest ( $P < 5 \times 10^{-8}$ ,  $r^2 < 0.01$ , and clump distance  $> 10,000$  kb) were chosen as instrument variables, using the 1000 Genomes Project as the reference panel. Detailed lists of instrument variables can be found in the supplemental figures. The inverse-variance weighted method was adopted as the main statistical method for

unadjusted analysis. This approach aggregates the Wald ratio estimates for each eligible SNP, as determined by dividing the SNP-outcome association by the SNP-exposure association. We also present results derived from the MR-Egger, weighted median simple mode and weighted mode methods. To ensure the robustness of our findings, we further conducted a series of sensitivity analyses including heterogeneity analysis, horizontal pleiotropy analysis, and leave-one-out analysis. All additional analyses are presented in the supplemental figures. A Benjamini–Hochberg adjusted  $P < 0.05$  was considered statistically significant to control for false discoveries while maintaining sensitivity.

### Single-Nucleus RNA Sequencing

Single-nucleus RNA sequencing (snRNA-seq) data analysis was performed using Seurat 4.4.0, except where other specifications were indicated.<sup>24</sup> Data from five kidney papillary tissues, including three normal controls and two calcium oxalate stone formers, as well as the processing codes were obtained from the Jain Lab.<sup>25,26</sup> For quality control, all mitochondrial transcripts were excluded, and doublets were identified and removed using Doublet-Detection software (<https://github.com/JonathanShor/DoubletDetection>). Only nuclei with gene counts ranging from 400 to 7500 were retained. To further refine the quality, a gene-to-unique molecular identifier ratio filter was applied using Pagoda2 (<https://github.com/hms-dbmi/pagoda2>). Total counts per nucleus were normalized, batch effects were corrected, and principal component analysis was conducted on the top 3000 significant variant genes. Cell type annotation was carried out in two steps: Cells were initially mapped to snCv3 with cortex tissue removed and then refined through manual annotation based on molecular markers.<sup>25</sup> Adaptive, degenerative,

and undifferentiated cells were removed from the analysis. The differential expression for each cell type was calculated using the Wilcoxon test with Bonferroni correction. Differentially expressed genes were defined as those with  $\log_2FC > 0.5$  and adjusted  $P < 0.05$ .

### Statistical Analysis

Continuous data are presented as mean $\pm$ SD or median with interquartile range, based on their distribution determined by the Shapiro–Wilk test for normality. For comparisons between two independent groups,  $t$  tests were applied to normally distributed data, whereas the Wilcoxon rank-sum test was used for non-normally distributed data. Categorical variables were reported as counts (percentages), and their associations were analyzed using the chi-squared test. For correlation analysis, Pearson correlation was used for normally distributed data, whereas Spearman correlation was applied to non-normally distributed data. The concentration-response analysis was conducted to examine the relationship between kidney stone risk and blood protein concentrations of interest using a generalized additive model, adjusting for age, sex, eGFR, and BMI. All statistical analyses were performed using R 4.2.3 (R Core Team, Vienna, Austria). A two-tailed  $P < 0.05$  was considered statistically significant.

## Results

### Clinical Characteristics of the UKBB Cohort

The overall workflow of this study is shown in Figure 1. The expression levels of 2922 blood proteins were compared between UKBB stone formers ( $n=626$ ) and controls ( $n=34,705$ ). Clinical characteristics of the stone formers versus controls are presented in Table 2. Patients with kidney stones were more commonly male (70% versus 45%), had a higher BMI (median difference: 1.4 kg/m<sup>2</sup>), and a higher prevalence of type 2 diabetes

(19% versus 7%) and hypertension (49% versus 32%), whereas eGFR was similar to controls (Table 2). In the age-adjusted and sex-adjusted multivariable model, patients with kidney stone exhibited a higher prevalence of 29 comorbidities, including obesity, diabetes, and hypertension (Supplemental Table 1).

### Differentially Expressed Proteins in Kidney Stone Patients

A total of 243 significantly altered proteins were identified with a Bonferroni-adjusted  $P < 0.05$  and  $\log_2FC > 0.07$  in unadjusted analysis (Figure 2 and Supplemental Table 2). In a multivariable model that adjusted for clinical characteristics and 14 nonurinary system comorbidities (Supplemental Table 1), only nine proteins remained significantly associated with kidney stones (Figure 2). Of these, seven were upregulated, including scavenger receptor cysteine-rich domain-containing group B protein (SSC4D;  $\beta$ , 0.28; 95% confidence interval [CI], 0.17 to 0.38), S100 calcium-binding protein G (S100G;  $\beta$ , 0.11; 95% CI, 0.07 to 0.16), and SPP1 ( $\beta$ , 0.10; 95% CI, 0.06 to 0.14), whereas two were downregulated: UMOD ( $\beta$ ,  $-0.10$ ; 95% CI,  $-0.15$  to  $-0.05$ ) and dopa decarboxylase (DDC;  $\beta$ ,  $-0.11$ ; 95% CI,  $-0.15$  to  $-0.06$ ; Figure 2). Pathway enrichment analysis revealed that the differentially expressed proteins identified from the multivariable analysis were predominantly enriched in extracellular matrix (ECM) organization (adjusted  $P = 0.025$ ) and degradation of ECM (adjusted  $P = 0.014$ ) pathways (Figure 2).

### Causal Relationship between Plasma Proteins and Kidney Stones

UKBB GWAS data for differentially expressed proteins identified in the multivariable analysis were used for further analysis (Figure 3 and Supplemental Figure 1). When the FinnGen kidney stone GWAS data were used as an exposure, a history of kidney stones was associated with higher blood concentrations of matrix metalloproteinase 7 (MMP7;  $\beta$ , 0.05; 95% CI, 0.02 to 0.08) and S100G ( $\beta$ , 0.09;

**Table 2. Baseline characteristics for participants in the proteomics study from the UK Biobank**

Characteristic <sup>a</sup>	Without Kidney Stones ( $n=34,705$ )	Kidney Stones ( $n=626$ )
Age, yr	58 (50–63)	58 (51–63)
Sex, No. (%)		
Female	19,135 (55)	186 (30)
Male	15,570 (45)	440 (70)
Smoking, No. (%)	20,467 (59)	380 (61)
Hypertension, No. (%)	11,063 (32)	305 (49)
Type 2 diabetes, No. (%)	2542 (7)	120 (19)
BMI, kg/m <sup>2</sup>	26.6 (24.1–29.7)	28.0 (25.4–30.8)
Systolic BP, mm Hg	136 (124–149)	140 (128–151)
Diastolic BP, mm Hg	82 (75–89)	84 (77–91)
Serum creatinine, mg/dl	0.79 (0.69–0.92)	0.86 (0.75–0.96)
eGFR, ml/min per 1.73 m <sup>2</sup>	97 (87–104)	96 (87–104)
Uric acid, mg/dl	5.0 (4.1–6.0)	5.5 (4.6–6.3)
Total cholesterol, mg/dl	219 (190–249)	214 (187–242)
Triglycerides, mg/dl	129 (92–185)	147 (105–222)
LDL, mg/dl	136 (114–159)	135 (112–156)
HDL, mg/dl	55 (46–65)	48 (41–58)
HbA1c, %	5.4 (5.1–5.6)	5.4 (5.2–5.7)

BMI, body mass index; HbA1c, hemoglobin A1c.

<sup>a</sup>Median (interquartile range); No. (%).



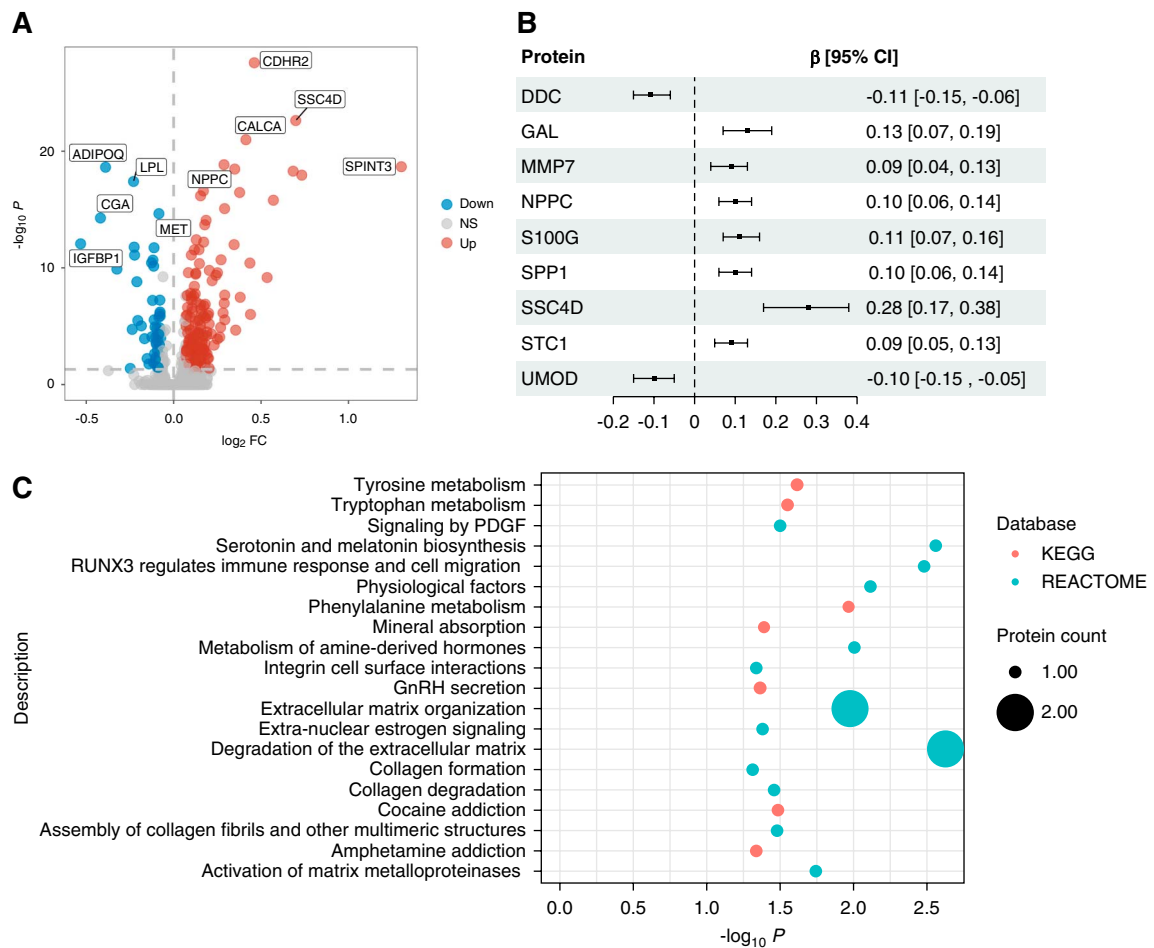


**Figure 2. Differentially expressed proteins among kidney stone formers in the UKBB.** (A) Volcano plot showing 243 proteins were significantly associated with kidney stones (189 upregulated; 54 downregulated) in the unadjusted analysis. The top five upregulated and downregulated proteins with the lowest  $P$  values are labeled. (B) Forest plot showing the nine proteins independently associated with kidney stones. The  $\beta$  value represents the effect of a kidney stone diagnosis on protein concentration measured in NPX units, where a one-unit higher represents a doubling of the absolute concentration. (C) Enrichment analysis of the nine proteins using KEGG and Reactome databases. CI, confidence interval; DDC, dopa decarboxylase; FC, fold change; GAL, galanin; GnRH, gonadotropin-releasing hormone; KEGG, Kyoto Encyclopedia of Genes and Genomes; MMP7, matrix metalloproteinase 7; NPPC, natriuretic peptide C; NPX, normalized protein eXpression; NS, not significant; S100G, S100 calcium-binding protein G; SPP1, secreted phosphoprotein 1 (also known as osteopontin); SSC4D, scavenger receptor cysteine-rich domain-containing group B protein; STC1, stanniocalcin 1; UMOD, uromodulin.

95% CI, 0.03 to 0.15; Figure 4 and Supplemental Figures 2 and 3).

Independent cis-pQTLs located within  $\pm 500$  kb of the encoding gene were then used as instrumental variables to examine their effects on kidney stone risk (Figure 3). UMOD (OR, 0.93; 95% CI, 0.90 to 0.97) and SSC4D (OR, 1.10; 95% CI, 1.02 to 1.18) were significantly associated with kidney stone risk, whereas DDC (OR, 0.92; 95% CI, 0.85 to 0.99) demonstrated a borderline significant negative association (Figure 4 and Supplemental Figures 4 and 5). Stanniocalcin 1 was not included in the analysis because of an insufficient number of qualified instrumental variables.

Next, we conducted a kidney stone GWAS among participants of the MCBB (kidney stone prevalence: 14%; 5998 cases and 37,746 controls), which identified a genome-wide significant signal near the *CLDN14* gene (Figure 5 and Table 1). The baseline characteristics of the MCBB

cohort are provided in Supplemental Table 3. In a validation MR analysis using kidney stone GWAS data from the MCBB, UMOD was associated with a lower risk (OR, 0.92; 95% CI, 0.86 to 0.98) and SSC4D (OR, 1.13; 95% CI, 1.01 to 1.27) with a higher risk of kidney stones (Figure 5 and Supplemental Figures 6 and 7). However, DDC (OR, 0.95; 95% CI, 0.87 to 1.04) did not retain a significant association with the kidney stone phenotype (Figure 5). All MR analyses demonstrated no significant pleiotropy or heterogeneity, except for the effect of kidney stones on blood S100G, in which case significant heterogeneity was observed (Cochrane  $Q=88.9$ ,  $P < 0.001$ ; Supplemental Figures 2–7).

Finally, the adjusted concentration-response relationship between blood UMOD and SSC4D levels and kidney stone risk was assessed using generalized additive models. After adjusting for age, sex, eGFR, and BMI, kidney stone risk in the UKBB increased in a concentration-dependent

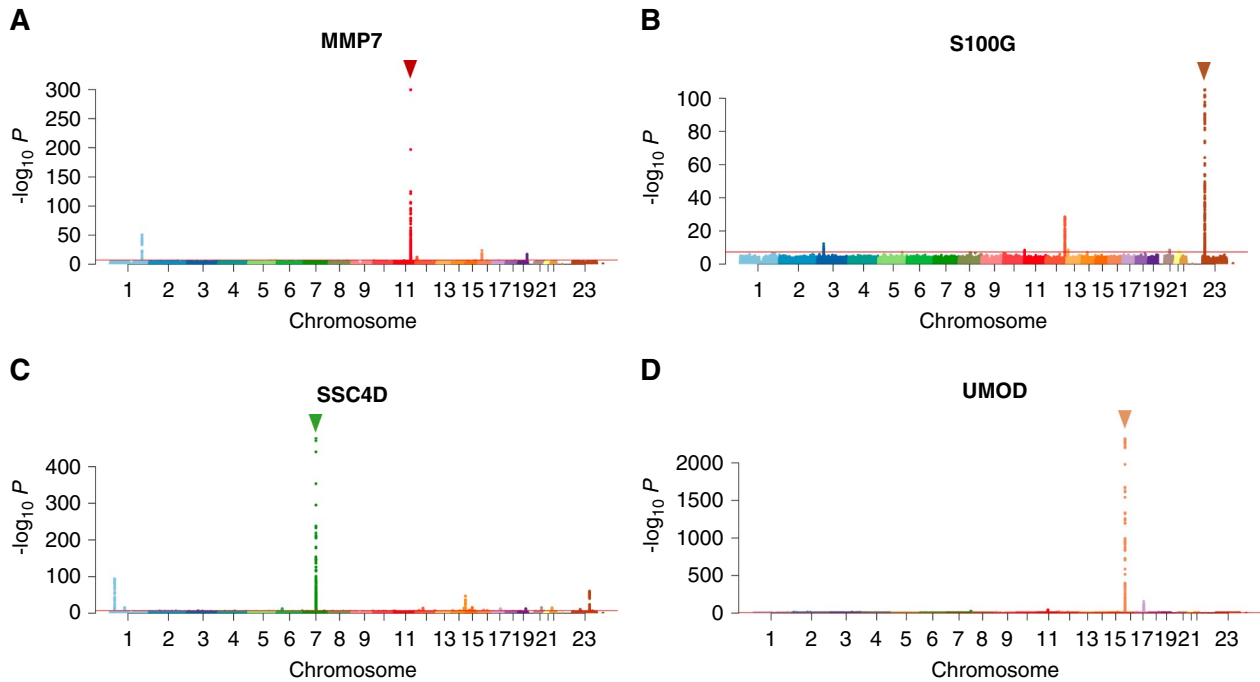


**Figure 3. GWAS and pQTL analysis of the selected blood proteins in the UKBB.** Manhattan plots depicting GWAS for (A) MMP7 (chromosome 11q22.2), (B) S100G (chromosome Xp22.2), (C) SSC4D (chromosome 7q11.23), and (D) UMOD (chromosome 16p12.3) in the UKBB. A genome-wide significance threshold of  $P < 5 \times 10^{-8}$  was applied. The arrowheads highlight the cis-pQTLs associated with each GWAS, identifying significant genetic regions near the encoding gene that influence the blood levels of these proteins. pQTL, protein quantitative trait locus.

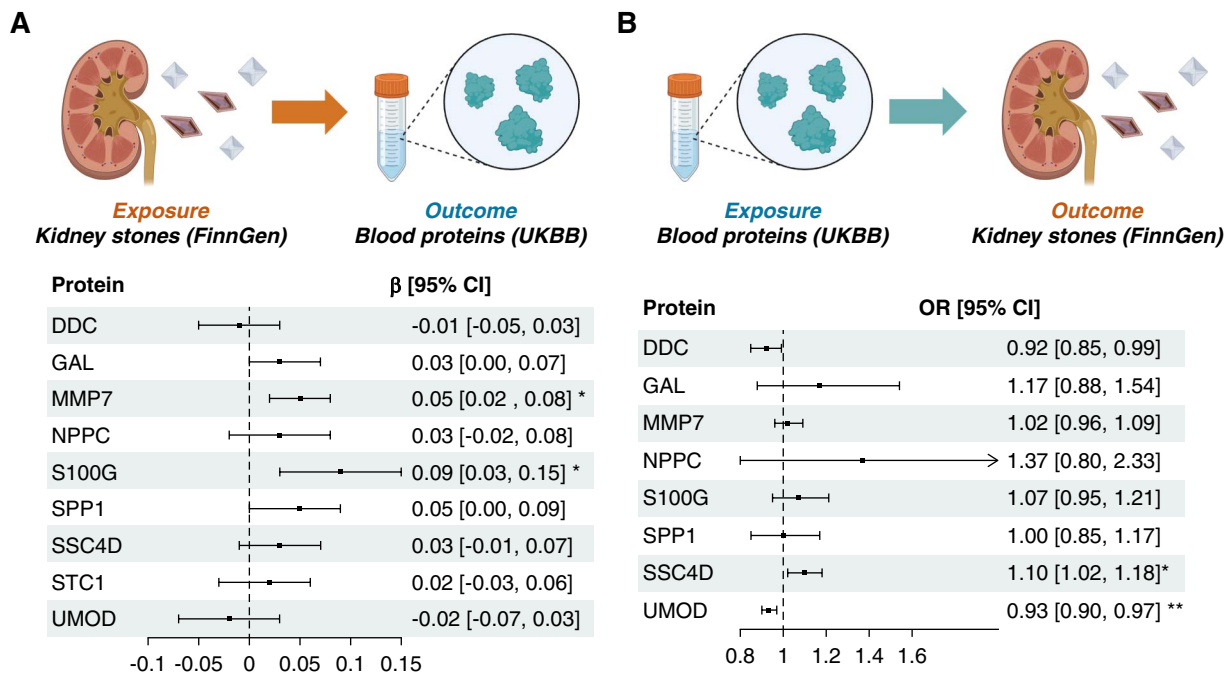


**Figure 4. MR analysis for kidney stones and differentially expressed blood proteins.** (A) MR analysis between FinnGen kidney stone GWAS (exposure) and UKBB protein GWAS (outcome). (B) MR analysis between UKBB protein GWAS (exposure) and FinnGen kidney stone GWAS (outcome). STC1 was excluded from the analysis because of an insufficient number of qualified instrumental variables. \*Adjusted  $P < 0.05$ ; \*\*adjusted  $P < 0.01$ . OR, odds ratio.

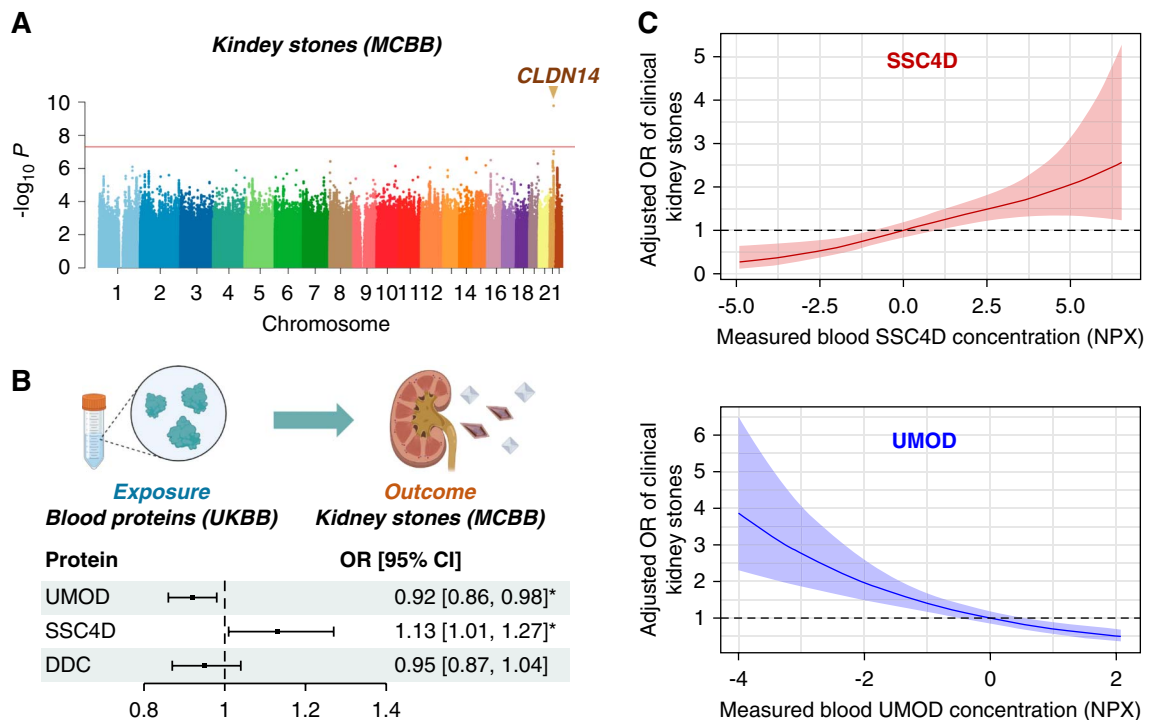


**Figure 5. Validation MR in the MCBB and concentration-response analysis in the UKBB.** (A) Manhattan plot for the MCBB kidney stone GWAS. The arrowhead indicates the genome-wide significant signal ( $P < 5 \times 10^{-8}$ ) near the *CLDN14* gene. (B) MR analysis between UKBB protein GWAS (exposure) and MCBB kidney stone GWAS (outcome). (C) Concentration-response analysis of UMOD and SSC4D with kidney stone risk in the UKBB, performed using adjusted generalized additive models. Protein concentrations are presented in NPX units, where a one-unit higher represents a doubling of the absolute concentration. \*Adjusted  $P < 0.05$ .

manner with higher plasma SSC4D levels and lower plasma UMOD levels (Figure 5).

#### snRNA-Seq Analysis of the Human Kidney Papilla

Next, the mRNA expression levels of MMP7, S100G, UMOD, and SSC4D were validated using kidney papillary snRNA-seq data from 23,427 nuclei obtained from two calcium oxalate stone formers and three controls. Notably, UMOD mRNA expression was significantly reduced in the thick ascending limb (TAL) of the stone formers, which is the primary site of renal UMOD synthesis and secretion ( $\log_2\text{FC} = -0.94$ , adjusted  $P < 0.001$ ; Figure 6). Conversely, expression of MMP7 was increased in TAL cells ( $\log_2\text{FC} = 0.92$ , adjusted  $P < 0.001$ ) and myofibroblast cells ( $\log_2\text{FC} = 0.52$ , adjusted  $P < 0.05$ ) of stone formers, with no significant changes in other tubular cell types (Supplemental Figure 8). However, the mRNA expression levels of S100G and SSC4D were relatively low in the kidney papilla, with no significant variations detected across all cell types (Supplemental Figure 8).

#### Quantitative Trait Loci Correlation Analysis

The correlation between the effects of genetic variants on blood protein levels and renal tubule mRNA expression was analyzed to determine whether changes in blood protein concentrations corresponded to those in renal mRNA expression. Analysis of published expression quantitative trait loci data for human kidney tubules

( $N=121$ )<sup>27</sup> revealed a significant correlation between genetic effects on blood UMOD concentration and tubular UMOD mRNA expression (Pearson  $r=0.68$ ; 95% CI, 0.33 to 0.90) using independent cis-pQTLs with a linkage disequilibrium  $r^2 < 0.2$  (Figure 6). However, the correlation for MMP7 was NS (Pearson  $r=0.08$ ; 95% CI,  $-0.33$  to  $0.66$ ; Supplemental Figure 9). No significant expression quantitative trait loci were found in renal tubules for S100G and SSC4D.

Because most UMOD produced by the TAL is excreted into urine, we also performed a cis-pQTL analysis using publicly available urinary UMOD GWAS data from 29,315 European patients (Table 1). A consistent and strong correlation was observed between the effects of genetic variants on blood and urinary UMOD levels (urinary concentration: Pearson  $r=0.88$ ; 95% CI, 0.82 to 0.92; urinary UMOD/creatinine ratio: Pearson  $r=0.91$ ; 95% CI, 0.87 to 0.94; Figure 6).

#### Independent Association between UMOD and Kidney Stones

To investigate whether the effect of UMOD on kidney stone risk was mediated by kidney function, we conducted additional analyses in the UKBB GWAS adjusting for eGFR (Table 1). SNPs near the *UMOD* gene exhibited very similar effect patterns on kidney stones with or without eGFR adjustment (lead SNP in standard GWAS: rs77924615 [G>A]; OR, 1.24; 95% CI, 1.19 to 1.29; lead SNP in eGFR-adjusted GWAS: rs77924615 [G>A]; OR, 1.25; 95%



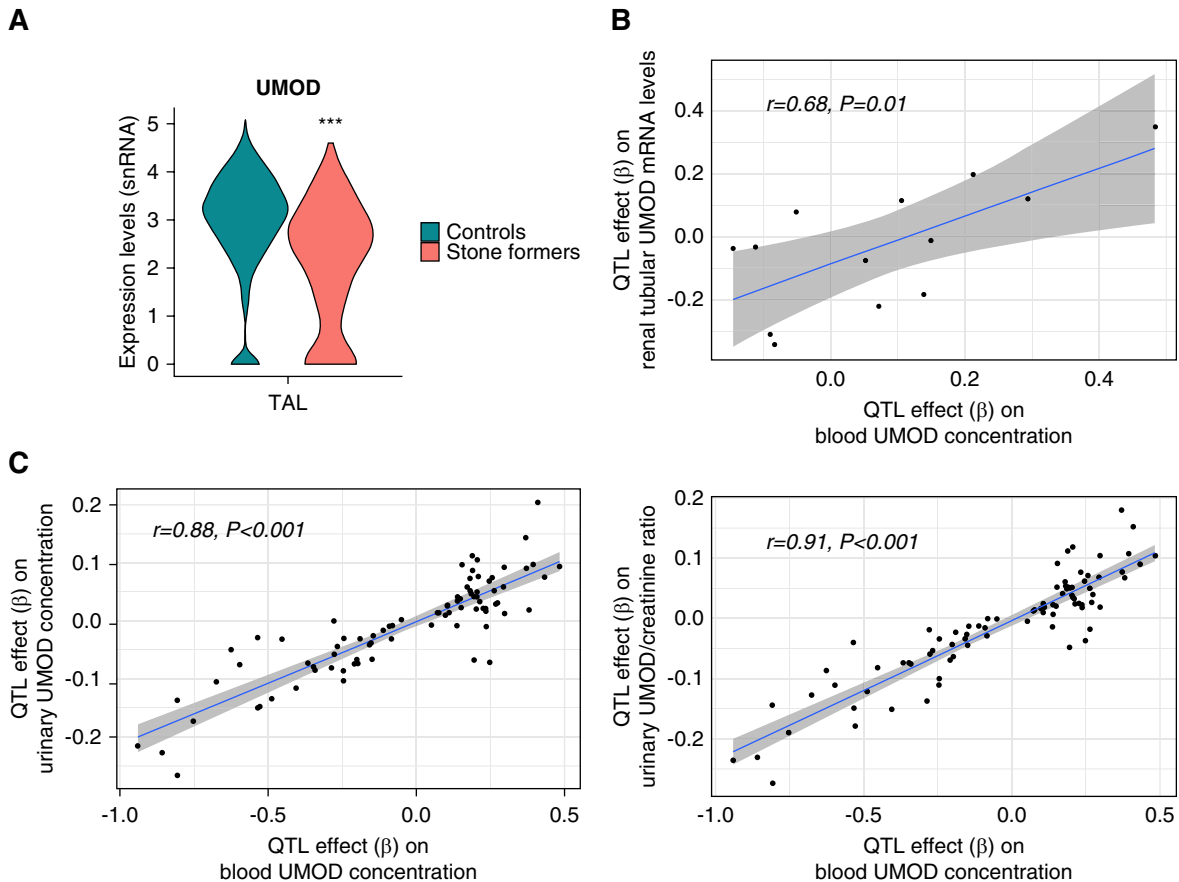


**Figure 6. snRNA-seq and QTL correlation analysis of UMOD.** (A) snRNA-seq analysis showing significantly decreased UMOD in the TAL. (B) QTL correlation analysis between blood protein and renal tubular mRNA levels for UMOD. (C) QTL correlation analysis between blood and urinary UMOD levels (with or without correction for urinary creatinine). In QTL correlation panels, each dot represents an independent genetic variant, and the  $\beta$  value indicates its effect on UMOD expression. \*\*\*Adjusted  $P < 0.001$ . snRNA-seq, single-nucleus RNA sequencing; TAL, thick ascending limb.

CI, 1.20 to 1.30; Figure 7). Furthermore, colocalization between plasma UMOD concentration and a kidney stone phenotype was observed within the *UMOD* gene (PPH4=0.90) and near the rs77924615 region ( $\pm 50$  kb, PPH4=0.84) after adjusting for eGFR.

## Discussion

Here, we present results from a comprehensive multiomics study of independent associations between plasma proteins and kidney stone disease. After robust adjustment in multivariable analysis, nine proteins were independently dysregulated in the context of kidney stones (upregulated: SSC4D, MMP7, S100G, SPP1, galanin, natriuretic peptide C, stanniocalcin 1; downregulated: UMOD, DDC). Notably, none of the significant findings from previous genome-wide MR analyses overlapped with these proteins.<sup>12,13</sup> Pathway enrichment analysis highlighted their primary involvement in ECM pathways, consistent with previous publications.<sup>28–30</sup>

The current results using MR analysis to infer causation between exposure and outcome suggest that a history of kidney stones is associated with elevated blood concentra-

tions of MMP7 and S100G. A recent cross-sectional study also demonstrated upregulation of renal and urinary MMP7 in calcium oxalate stone formers.<sup>26</sup> Intrarenal expression of MMP7 in humans positively correlates with macrophage infiltration, which may, in turn, facilitate crystal dissolution.<sup>31</sup> S100G, also known as calbindin-D9k, is a calcium-binding protein primarily expressed in the intestine.<sup>32</sup> Although its family members calgranulin A (S100A8) and calgranulin B (S100A9) are known components of kidney stone matrices,<sup>33</sup> the role of S100G in kidney stone formation remains poorly defined. Our MR analysis revealed that the blood concentrations of these two plasma proteins were not associated with kidney stone risk, suggesting they are more likely consequences of stone formation or kidney stone-related pathophysiological changes rather than causal factors.

Conversely, this study showed that higher blood UMOD concentrations were significantly associated with reduced kidney stone risk. Over many decades, UMOD, the most abundant protein in normal human urine, has been extensively studied in the context of kidney stone disease, urinary tract infection, CKD, and tubular interstitial disease.<sup>34,35</sup> UMOD is predominantly excreted into the

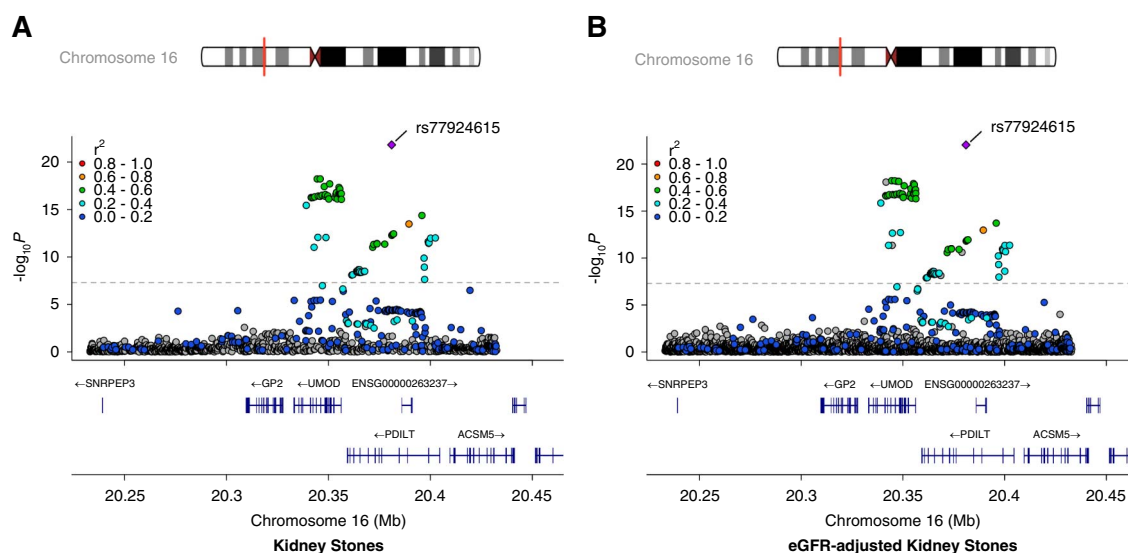


**Figure 7. Regional association of kidney stones and UMOD-related SNPs in the UKBB.** LocusZoom plots illustrating the genetic association with kidney stones (A) before and (B) after baseline eGFR adjustment.  $r^2$  values are color-coded to indicate the strength of LD between other genetic variants and the lead SNPs (represented by purple diamonds). The gray dotted line denotes the genome-wide significance threshold of  $P < 5 \times 10^{-8}$ . ACSM5, acyl-CoA synthetase medium chain family member 5; LD, linkage disequilibrium; PDILT, protein disulfide isomerase like, testis expressed; SNP, single-nucleotide polymorphism; SNRPEP3, small nuclear ribonucleoprotein E pseudogene 3.

urine by the epithelial cells lining the TAL and to a lesser extent by cells in the early distal convoluted tubule. UMOD is also present at the basolateral membrane of TAL cells, where it is released into the kidney interstitium and the systemic circulation, although in much smaller amounts than those excreted into urine.<sup>34</sup> Experimental studies suggest urinary UMOD might play a protective role against kidney stone formation by inhibiting crystal aggregation and enhancing calcium reabsorption.<sup>36–39</sup> However, observational studies have reported conflicting findings regarding urinary UMOD levels in stone formers.<sup>40–42</sup> These discrepancies may stem from the highly variable nature of urinary UMOD. Multiple factors such as water intake, sample centrifugation, storage conditions, and the polymerization state of UMOD can significantly affect its accurate measurements.<sup>43,44</sup> Consequently, despite similar effects of genetic variants on urinary and blood UMOD levels, only weak-to-moderate correlations are observed between their levels in clinical settings.<sup>43,45</sup> In addition, within the urinary system, the structure and function of UMOD are significantly influenced by factors such as ionic strength, pH, and post-translational modifications (*e.g.*, oxidative changes), which may potentially shift its role from inhibiting to promoting kidney stone formation.<sup>46,47</sup>

Given these considerations, measuring circulating UMOD concentrations offers several advantages over urinary UMOD, including greater stability. Blood UMOD predominantly exists in a nonpolymerized form, and the pH and ionic strength of blood remain relatively consistent across individuals, unlike the highly variable conditions found in urine.<sup>44</sup> Importantly, our quantitative trait locus correlation analysis suggests that circulating UMOD reliably reflects its intrarenal expression. Circulating UMOD concentration has been widely studied over recent years as

a novel biomarker of kidney injury and cardiovascular disease.<sup>44,45</sup> However, the relationship between blood UMOD concentration and kidney stone disease remains largely unknown. Our findings, including concentration-response analysis and eGFR-adjusted GWAS, provide robust evidence to support the association between circulating UMOD and kidney stone risk. Importantly, this relationship is independent of CKD status, a condition that has also been associated with both UMOD concentration and kidney stone formation.<sup>44,48,49</sup> Furthermore, recent studies indicate that circulating UMOD inhibits systemic oxidative stress.<sup>50,51</sup> Whether the effects of UMOD on oxidative stress contribute to its protective role regarding kidney stone risk remains to be clarified.

Increased SSC4D, a scavenger receptor highly expressed in macrophages, was also identified as a novel marker for kidney stone risk, which has not been reported previously.<sup>52</sup> SSC4D emerged as the most upregulated protein in our multivariable proteomics analysis and demonstrated consistent associations with kidney stone risk in both MR and concentration-response analyses. SSC4D primarily functions as a pattern recognition receptor.<sup>53</sup> Given the emerging role for macrophages and other pattern recognition receptors such as Toll-like receptors in renal processing of crystals and kidney stone formation, a role for SSC4D in the inflammatory response to crystals suggests a plausible hypothesis that merits further study.<sup>31,54</sup> Interestingly, a recent study found that circulating SSC4D was also associated with fat mass index in a cohort of 4950 Swedish women, suggesting its potential role in metabolic regulation.<sup>55</sup> Further research is needed to elucidate the underlying mechanisms of SSC4D in kidney stone formation and its potential as a biomarker for kidney stone risk.

This study has several limitations. In both the UKBB and MCBB, kidney stone status was defined using

electronic medical records rather than computed tomography imaging, which may introduce misclassification bias. It is likely that these diagnosis codes are not consistently applied when stones are incidental, small, or asymptomatic on imaging. Despite this lack of sensitivity, presumably for smaller and more incidental stones, we still observed significant associations with kidney stone disease. Future studies incorporating computed tomography-based definitions are warranted to more accurately characterize this association. Second, although multiple corrections and rigorous adjustments were applied to enhance the robustness of our study, this approach may have higher risk of false negatives. Third, as the study primarily analyzed data from populations of European ancestry, the findings may not fully generalize to other ethnic groups. Fourth, although MR analysis in this cross-sectional study aims to infer causality, the use of relatively weaker instrumental variables, such as those identified in the SSC4D GWAS compared with UMOD, along with the potential for undetected pleiotropy, may limit the robustness of causal claims. Prospective longitudinal studies are still required to validate whether plasma protein levels can predict the incidence of kidney stones. Moreover, as UKBB only provides proteomics data measured using a relative quantification technique, future studies using validated assays to measure actual concentrations and to establish appropriate reference values are warranted. Finally, owing to the unavailability of data, our study did not account for the type, severity, or recurrence of kidney stones, and the results only reflect the general association between kidney stones and circulating proteins.

Despite its limitations, this study has several strengths. Most notably, the integration of large multiomics datasets with an extensive and rigorous analytical approach enables the reliable identification of associations with kidney stone disease. Although some of these proteins appear to be consequences rather than causes of kidney stones, blood UMOD and SSC4D levels were associated with kidney stone risk, even after adjusting for comorbidities, particularly CKD/eGFR. Furthermore, this study provides a strong rationale to use blood UMOD as a more reliable biomarker to reflect urinary UMOD excretion to understand associations with diseases like kidney stone formation. Overall, this study highlights the need for renewed research into the potential role of UMOD and SSC4D in the pathogenesis and prognosis of kidney stone disease.

## Disclosures

Disclosure forms, as provided by each author, are available with the online version of the article at <http://links.lww.com/JSN/F299>.

## Author Contributions

**Conceptualization:** John C. Lieske.

**Data curation:** Isaac W. Stark, Le-Ting Zhou.

**Formal analysis:** Le-Ting Zhou.

**Funding acquisition:** Muthuvel Jayachandran, John C. Lieske, Le-Ting Zhou.

**Investigation:** Isaac W. Stark, Le-Ting Zhou.

**Methodology:** Muthuvel Jayachandran, Nicholas B. Larson, Shannon K. McDonnell, Andrew D. Rule, Le-Ting Zhou.

**Project administration:** Peter C. Harris.

**Resources:** John C. Lieske.

**Software:** Nicholas B. Larson, Shannon K. McDonnell.

**Supervision:** Peter C. Harris.

**Validation:** Andrew D. Rule, Isaac W. Stark, Le-Ting Zhou.

**Writing – original draft:** Isaac W. Stark, Le-Ting Zhou.

**Writing – review & editing:** Peter C. Harris, Muthuvel Jayachandran, Kevin Koo, Nicholas B. Larson, John C. Lieske, Shannon K. McDonnell, Andrew D. Rule, Isaac W. Stark, Le-Ting Zhou.

## Funding

J.C. Lieske: National Institute of Diabetes and Digestive and Kidney Diseases (DK100227, DK83007, DK133171, and DK135097). L.-T. Zhou: Wuxi Health and Family Planning Commission (HB2023010). M. Jayachandran: National Institute of Diabetes and Digestive and Kidney Diseases (DK135097 and DK132046). This work was supported by Rochester Epidemiology Project from the National Institutes of Health, US Public Health Service (AG034676) and Top Talent Support Program for young and middle-aged people of Wuxi Health Committee (HB2023010).

## Acknowledgments

The contents are solely the responsibility of the authors and do not necessarily represent the official views of the National Institutes of Health. Funders did not have a role in study design, data collection, analysis, reporting, or decision to submit for publication.

## Data Availability Statements

The following datasets have been uploaded to Figshare. eGFR-adjusted kidney stone GWAS summary statistics in the UKBB: <https://figshare.com/s/20bb20917800782761dc> Standard kidney stone GWAS summary statistics in the UKBB: <https://figshare.com/s/cd271363489008737819> Standard kidney stone GWAS summary statistics in the MCB: <https://figshare.com/s/60de67d231353556520e>.

## Supplemental Material

This article contains the following supplemental material online at <http://links.lww.com/JSN/F300>.

**Supplemental Table 1.** Comorbidities associated with kidney stones in the age-adjusted and sex-adjusted multivariable model.

**Supplemental Table 2.** Unadjusted analysis of differentially expressed blood proteins in patients with kidney stone.

**Supplemental Table 3.** Baseline characteristics for participants from the MCB.

**Supplemental Figure 1.** GWAS and pQTL analysis of the selected blood proteins in the UKBB.

**Supplemental Figure 2.** MR analysis of the influence of kidney stones on blood MMP7 in the FinnGen (exposure)/UKBB (outcome) datasets.

**Supplemental Figure 3.** MR analysis of the influence of kidney stones on blood S100G in the FinnGen (exposure)/UKBB (outcome) datasets.

**Supplemental Figure 4.** MR analysis of the influence of blood SSC4D on kidney stones in the UKBB (exposure)/FinnGen (outcome) datasets.

**Supplemental Figure 5.** MR analysis of the influence of blood UMOD on kidney stones in the UKBB (exposure)/FinnGen (outcome) datasets.

**Supplemental Figure 6.** MR analysis of the influence of blood SSC4D on kidney stones in the UKBB (exposure)/MCBB (outcome) datasets.

**Supplemental Figure 7.** MR analysis of the influence of blood UMOD on kidney stones in the UKBB (exposure)/MCBB (outcome) datasets.

**Supplemental Figure 8.** Single-nucleus RNA analysis of mRNA expression of MMP7, S100G, and SSC4D in kidney papillary tissues.

**Supplemental Figure 9.** Quantitative trait locus correlation analysis between blood protein levels and renal tubular mRNA expression for MMP7.

**Supplemental Method 1.** ICD-10 codes used to identify infection in the UKBB.

**Supplemental Method 2.** Genotyping methods in the MCBB.

**Supplemental Method 3.** Electronic definition of kidney stone cases and controls in the MCBB.

## References

- Sorokin I, Mamoulakis C, Miyazawa K, Rodgers A, Talati J, Lotan Y. Epidemiology of stone disease across the world. *World J Urol.* 2017;35(9):1301–1320. doi:10.1007/s00345-017-2008-6
- Singh P, Enders FT, Vaughan LE, et al. Stone composition among first-time symptomatic kidney stone formers in the community. *Mayo Clin Proc.* 2015;90(10):1356–1365. doi:10.1016/j.mayocp.2015.07.016
- Coe FL, Worcester EM, Evan AP. Idiopathic hypercalciuria and formation of calcium renal stones. *Nat Rev Nephrol.* 2016;12(9):519–533. doi:10.1038/nrneph.2016.101
- Glover LM, Bass MA, Carithers T, Loprinzi PD. Association of kidney stones with atherosclerotic cardiovascular disease among adults in the United States: considerations by race-ethnicity. *Physiol Behav.* 2016;157:63–66. doi:10.1016/j.physbeh.2016.01.026
- Drozdz D, Alvarez-Pitti J, Wójcik M, et al. Obesity and cardiometabolic risk factors: from childhood to adulthood. *Nutrients.* 2021;13(11):4176. doi:10.3390/nu13114176
- Hales CM, Fryar CD, Carroll MD, Freedman DS, Ogden CL. Trends in obesity and severe obesity prevalence in US youth and adults by sex and age, 2007–2008 to 2015–2016. *JAMA.* 2018;319(16):1723–1725. doi:10.1001/jama.2018.3060
- Spivacow FR, Del Valle EE, Lores E, Rey PG. Kidney stones: composition, frequency and relation to metabolic diagnosis. *Medicina (B Aires).* 2016;76(6):343–348. PMID: 27959841
- Pearle MS, Calhoun EA, Curhan GC.; Urologic Diseases of America Project. Urologic diseases in America project: urolithiasis. *J Urol.* 2005;173(3):848–857. doi:10.1097/01.ju.0000152082.14384.d7
- Pan W, Yun T, Ouyang X, et al. A blood-based multi-omic landscape for the molecular characterization of kidney stone disease. *Mol Omics.* 2024;20(5):322–332. doi:10.1039/D3MO00261F
- Kovacevic L, Kovacevic N, Lakshmanan Y. Proteomic analysis of inhibitory protein profiles in the urine of children with nephrolithiasis: implication for disease prevention. *Int Urol Nephrol.* 2022;54(11):2783–2788. doi:10.1007/s11255-022-03310-5
- Kaneko K, Kobayashi R, Yasuda M, Izumi Y, Yamanobe T, Shimizu T. Comparison of matrix proteins in different types of urinary stone by proteomic analysis using liquid chromatography-tandem mass spectrometry. *Int J Urol.* 2012;19(8):765–772. doi:10.1111/j.1442-2042.2012.03005.x
- Liang Z, Hu C, Pang H, Sha Y, Yao L, Liu F. Identifying therapeutic targets for kidney stone disease through proteome-wide Mendelian randomization and colocalization analysis. *Urolithiasis.* 2024;52(1):167. doi:10.1007/s00240-024-01669-x
- Wang L, Li KP, Chen SY, Wan S, Li XR, Yang L. Proteome-wide Mendelian randomization identifies therapeutic targets for nephrolithiasis. *Urolithiasis.* 2024;52(1):126. doi:10.1007/s00240-024-01627-7
- Sun BB, Chiou J, Traylor M, et al. Plasma proteomic associations with genetics and health in the UK Biobank. *Nature.* 2023;622(7982):329–338. doi:10.1038/s41586-023-06592-6
- Purcell S, Neale B, Todd-Brown K, et al. PLINK: a tool set for whole-genome association and population-based linkage analyses. *Am J Hum Genet.* 2007;81(3):559–575. doi:10.1086/519795
- Mbatchou J, Barnard L, Backman J, et al. Computationally efficient whole-genome regression for quantitative and binary traits. *Nat Genet.* 2021;53(7):1097–1103. doi:10.1038/s41588-021-00870-7
- Inker LA, Eneanya ND, Coresh J, et al. New creatinine- and cystatin C-based equations to estimate GFR without race. *N Engl J Med.* 2021;385(19):1737–1749. doi:10.1056/NEJMoa2102953
- Kurki MI, Karjalainen J, Palta P, et al. FinnGen provides genetic insights from a well-phenotyped isolated population. *Nature.* 2023;613(7944):508–518. doi:10.1038/s41586-022-05473-8
- Joseph CB, Mariniello M, Yoshifuji A, et al. Meta-GWAS Reveals novel genetic variants associated with urinary excretion of uromodulin. *J Am Soc Nephrol.* 2022;33(3):511–529. doi:10.1681/ASN.2021040491
- Wallace C. Eliciting priors and relaxing the single causal variant assumption in colocalisation analyses. *PLoS Genet.* 2020;16(4):e1008720. doi:10.1371/journal.pgen.1008720
- Yu G, Wang LG, Han Y, He QY. ClusterProfiler: an R package for comparing biological themes among gene clusters. *Omics.* 2012;16(5):284–287. doi:10.1089/omi.2011.0118
- Skrivankova VW, Richmond RC, Woolf BAR, et al. Strengthening the reporting of observational studies in Epidemiology using Mendelian randomization: the STROBE-MR statement. *JAMA.* 2021;326(16):1614–1621. doi:10.1001/jama.2021.18236
- Hemani G, Zheng J, Elsworth B, et al. The MR-Base platform supports systematic causal inference across the human phenotype. *Elife.* 2018;7:e34408. doi:10.7554/eLife.34408
- Hao Y, Hao S, Andersen-Nissen E, et al. Integrated analysis of multimodal single-cell data. *Cell.* 2021;184(13):3573–3587.e29. doi:10.1016/j.cell.2021.04.048
- Lake BB, Menon R, Winfree S, et al. An atlas of healthy and injured cell states and niches in the human kidney. *Nature.* 2023;619(7970):585–594. doi:10.1038/s41586-023-05769-3
- Canela VH, Bowen WS, Ferreira RM, et al. A spatially anchored transcriptomic atlas of the human kidney papilla identifies significant immune injury in patients with stone disease. *Nat Commun.* 2023;14(1):4140. doi:10.1038/s41467-023-38975-8
- Qiu C, Huang S, Park J, et al. Renal compartment-specific genetic variation analyses identify new pathways in chronic kidney disease. *Nat Med.* 2018;24(11):1721–1731. doi:10.1038/s41591-018-0194-4
- Hong S-Y, Xia Q-D, Xu J-Z, et al. Identification of the pivotal role of SPPI in kidney stone disease based on multiple bio-informatics analysis. *BMC Med Genomics.* 2022;15(1):7. doi:10.1186/s12920-022-01157-4
- Boonla C, Tosukhowong P, Pittau B, Schlosser A, Pimratana C, Kriegelstein K. Inflammatory and fibrotic proteins proteomically identified as key protein constituents in urine and stone matrix of patients with kidney calculi. *Clin Chim Acta.* 2014;429:81–89. doi:10.1016/j.cca.2013.11.036
- Khan S, Canales B, Dominguez-Gutierrez P. Randall's plaque and calcium oxalate stone formation: role for immunity and inflammation. *Nat Rev Nephrol.* 2021;17(6):417–433. doi:10.1038/s41581-020-00392-1
- Taguchi K, Okada A, Unno R, Hamamoto S, Yasui T. Macrophage function in calcium oxalate kidney stone formation: a systematic review of literature. *Front Immunol.* 2021;12:673690. doi:10.3389/fimmu.2021.673690
- Uhlén M, Fagerberg L, Hallström BM, et al. Proteomics. Tissue-based map of the human proteome. *Science.* 2015;347(6220):1260419. doi:10.1126/science.1260419
- Negri AL, Spivacow FR. Kidney stone matrix proteins: role in stone formation. *World J Nephrol.* 2023;12(2):21–28. doi:10.5527/wjn.v12.i2.21



34. Thielemans R, Speeckaert R, Delrue C, De Bruyne S, Oyaert M, Speeckaert MM. Unveiling the hidden power of uromodulin: a promising potential biomarker for kidney diseases. *Diagnostics (Basel)*. 2023;13(19):3077. doi:10.3390/diagnostics13193077
35. Mariniello M, Schiano G, Yoshifuji A, et al. Uromodulin processing in DNAJB11-kidney disease. *Kidney Int*. 2024;105(2):376–380. doi:10.1016/j.kint.2023.11.008
36. Liu Y, Mo L, Goldfarb DS, et al. Progressive renal papillary calcification and ureteral stone formation in mice deficient for Tamm-Horsfall protein. *Am J Physiol Renal Physiol*. 2010;299(3):F469–F478. doi:10.1152/ajprenal.00243.2010
37. Mo L, Liaw L, Evan AP, Sommer AJ, Lieske JC, Wu XR. Renal calcinosis and stone formation in mice lacking osteopontin, Tamm-Horsfall protein, or both. *Am J Physiol Renal Physiol*. 2007;293(6):F1935–F1943. doi:10.1152/ajprenal.00383.2007
38. Wolf MT, Wu XR, Huang CL. Uromodulin upregulates TRPV5 by impairing caveolin-mediated endocytosis. *Kidney Int*. 2013;84(1):130–137. doi:10.1038/ki.2013.63
39. Noonin C, Peerapen P, Yoodee S, Kapincharanon C, Kanlaya R, Thongboonkerd V. Systematic analysis of modulating activities of native human urinary Tamm-Horsfall protein on calcium oxalate crystallization, growth, aggregation, crystal-cell adhesion and invasion through extracellular matrix. *Chem Biol Interact*. 2022;357:109879. doi:10.1016/j.cbi.2022.109879
40. Jaggi M, Nakagawa Y, Zipperle L, Hess B. Tamm-Horsfall protein in recurrent calcium kidney stone formers with positive family history: abnormalities in urinary excretion, molecular structure and function. *Urol Res*. 2007;35(2):55–62. doi:10.1007/s00240-007-0083-7
41. Wai-Hoe L, Wing-Seng L, Ismail Z, Lay-Harn G. Proteomics and detection of uromodulin in first-time renal calculi patients and recurrent renal calculi patients. *Appl Biochem Biotechnol*. 2009;159(1):221–232. doi:10.1007/s12010-008-8503-x
42. Baggio B, Gambaro G, Favaro S, et al. Juvenile renal stone disease: a study of urinary promoting and inhibiting factors. *J Urol*. 1983;130(6):1133–1135. doi:10.1016/s0022-5347(17)51721-8
43. LaFavers KA, Gaddy AR, Micanovic R, et al. Water loading and uromodulin secretion in healthy individuals and idiopathic calcium stone formers. *Clin J Am Soc Nephrol*. 2023;18(8):1059–1067. doi:10.2215/CJN.0000000000000202
44. Nanamatsu A, de Araújo L, LaFavers KA, El-Achkar TM. Advances in uromodulin biology and potential clinical applications. *Nat Rev Nephrol*. 2024;20(12):806–821. doi:10.1038/s41581-024-00881-7
45. Ikeme JC, Scherzer R, Garimella PS, et al. The association of plasma and urine uromodulin with cardiovascular disease in persons with hypertension and CKD. *Am J Kidney Dis*. 2024;84(6):799–802. doi:10.1053/j.ajkd.2024.05.012
46. Hess B. Tamm-Horsfall glycoprotein--inhibitor or promoter of calcium oxalate monohydrate crystallization processes? *Urol Res*. 1992;20(1):83–86. doi:10.1007/bf00294343
47. Chaiyarit S, Thongboonkerd V. Oxidized forms of uromodulin promote calcium oxalate crystallization and growth, but not aggregation. *Int J Biol Macromol*. 2022;214:542–553. doi:10.1016/j.ijbiomac.2022.06.132
48. Zhou LT, Ali AE, Jayachandran M, et al. Association between kidney stones and CKD: a bidirectional Mendelian randomization study. *J Am Soc Nephrol*. 2024;35(12):1746–1757. doi:10.1681/ASN.0000000000000453
49. Akwo EA, Chen HC, Liu G, et al. Phenome-wide association study of UMOD gene variants and differential associations with clinical outcomes across populations in the million veteran program a multiethnic Biobank. *Kidney Int Rep*. 2022;7(8):1802–1818. doi:10.1016/j.ekir.2022.05.011
50. Steubl D, Schneider MP, Meiselbach H, et al. Association of serum uromodulin with death, cardiovascular events, and kidney failure in CKD. *Clin J Am Soc Nephrol*. 2020;15(5):616–624. doi:10.2215/CJN.11780919
51. LaFavers KA, Macedo E, Garimella PS, et al. Circulating uromodulin inhibits systemic oxidative stress by inactivating the TRPM2 channel. *Sci Transl Med*. 2019;11(512):eaaw3639. doi:10.1126/scitranslmed.aaw3639
52. Martínez VG, Moestrup SK, Holmskov U, Mollenhauer J, Lozano F. The conserved scavenger receptor cysteine-rich superfamily in therapy and diagnosis. *Pharmacol Rev*. 2011;63(4):967–1000. doi:10.1124/pr.111.004523
53. Cardoso MS, Santos RF, Almeida S, et al. Physical interactions with bacteria and Protozoan parasites establish the scavenger receptor SSC4D as a broad-spectrum pattern recognition receptor. *Front Immunol*. 2021;12:760770. doi:10.3389/fimmu.2021.760770
54. Olcucu MT, Teke K, Yalcin S, et al. Characterizing the association between toll-like receptor subtypes and nephrolithiasis with renal inflammation in an animal model. *Urology*. 2018;111:238.e1–238.e5. doi:10.1016/j.urology.2017.09.026
55. Titova OE, Brunius C, Warensjö Lemming E, et al. Comprehensive analyses of circulating cardiometabolic proteins and objective measures of fat mass. *Int J Obes (Lond)*. 2023;47(11):1043–1049. doi:10.1038/s41366-023-01351-z